

Color correction for Gabor deconvolution: a test with 2D synthetic data and field data

Peng Cheng, Gary F. Margrave and David C. Henley

ABSTRACT

Conventional deconvolution algorithms usually assume that the spectrum of reflectivity is white. However, the amplitude spectrum of reflectivity calculated from a well log usually demonstrates obvious dependence on frequency, which is referred to as the color of the reflectivity. Consequently, the white reflectivity assumption can lead to distortion of the deconvolution result. A practical color correction method for Gabor deconvolution has been proposed and tested on a synthetic 1D seismic trace. This article tests the proposed color correction method using a synthetic shot record and real field data. Testing on the synthetic shot record shows that color correction gives a better reflectivity estimation than conventional Gabor deconvolution, and can be successfully applied to shot records. Results of processing field data demonstrate that the seismic data have higher resolution and a better tie to the well log data when color correction is applied.

INTRODUCTION

Generally, deconvolution algorithms are based on the corresponding convolutional models, which separate a seismic trace into two parts representing the seismic wavelet and reflectivity respectively. Some assumptions are necessary to make deconvolution possible. First, the seismic wavelet is supposed to be minimum-phase. Then, the reflectivity is assumed to have a flat (white) amplitude spectrum over the deconvolution frequency band. Such a reflectivity is the so-called white reflectivity. However, in practice, the reflectivity is not white. In the Gabor transform domain, the amplitude spectrum of real reflectivity demonstrates a dependency on both time and frequency, which we refer as temporal and spectral color respectively. This indicates that the reflectivity color is time (actually depth) variant and needs to be corrected in a nonstationary way. Margrave and Lamoureux (2002) proposed a nonstationary Gabor deconvolution method, which makes the nonstationary correction to reflectivity convenient. Cheng and Margrave (2008) proposed a practical way to apply color correction for Gabor deconvolution when reference well log information is available. The Gabor spectrum of real reflectivity is approximated by low order polynomial curves with time-variant coefficients. This captures the reflectivity color effectively and is not overly sensitive to detail in the well log, which makes the information from regional well logs useful. Their testing on synthetic data showed that a deconvolved seismic trace with color correction has more accurate relative amplitude and smaller phase rotation compared to true reflectivity. In addition, Cheng and Margrave (2009) showed that the amplitude distortion and phase rotation of estimated reflectivity can result from temporal color and spectral color respectively.

The purpose of our work is to apply the color correction method to field data and to evaluate the results. This article briefly introduces the color correction method for

processing real data first. Then, the color correction method is evaluated using a synthetic shot record and field data. Finally, some conclusions are drawn from the examples.

COLOR CORRECTION FOR GABOR DECONVOLUTION

Cheng and Margrave (2008) proposed a color correction for Gabor deconvolution given by

$$R_G(\tau, f)_{est} = \frac{S_G(\tau, f) |R_G(\tau, f)|}{|S_G(\tau, f)| + \mu A_{max}} e^{i\varphi_c(\tau, f)}, \quad (1)$$

where $S_G(\tau, f)$ is the Gabor spectrum of seismic trace, $R_G(\tau, f)$ is the Gabor spectrum of the reflectivity calculated from the reference well log, μ is the stability factor (a small positive number roughly 10^{-4} , A_{max} is the maximum value of $|S_G(\tau, f)|$, and $\varphi_c(\tau, f)$ is given by the Hilbert transform (over frequency)

$$\varphi_c(\tau, f) = H(\ln | \frac{|R_G(\tau, f)|}{|S_G(\tau, f)| + \mu A_{max}} |). \quad (2)$$

Equation 2 is the usual Hilbert transform relation between amplitude and phase for a minimum phase filter but applied at each time of the Gabor spectrum. To apply the color correction to Gabor deconvolution, a smoothed Gabor amplitude spectrum of the reference reflectivity should be available. So, a non-detailed estimation of the time variant color feature of true reflectivity may be sufficient, which means the information of a regional well log can be applicable as well. Cheng and Margrave (2008) developed an effective way to approximate the Gabor amplitude spectral by using low order polynomial curves with time variant coefficients.

When applying the above color correction to field data, some practical issues should be considered. Usually, the available well log is incomplete (spans a smaller time range than the data), and needs to be aligned roughly with the field data. In addition, the amplitude of reflectivity may change significantly with depth/time. So, the color correction should address the alignment error properly. Cheng and Margrave (2009) separated the reflectivity color into temporal color and spectral color, which captures the time variant features and frequency variant features of the Gabor spectrum of reference reflectivity respectively, and showed that neglecting to correct for them can lead to relative amplitude distortion and phase rotation respectively. The spectral color correction, which can be regarded as normalized color correction, is probably more of interest from the point view of deconvolution.. Since the spectral color is not sensitive to the alignment error of well log to field data, spectral color correction may be preferable for prestack deconvolution. The spectral and temporal color correction can then be chosen for poststack deconvolution. The details about the implementation of color correction to field data using Promax is described by Henley et al (2010) in this volume.

EXAMPLES

The field example used to test our color correction method is a 2D seismic line with 159 shots and 151 receiver stations, which was acquired over Blackfoot field near Strathmore, Alberta in 1995. The reference well log is well 14-09 with a recorded depth

range from 218m to about 1700m, and which is about 600 meters away from the seismic line and can be projected to the seismic line using the X-Y coordinates.

The density log, P wave velocity log, computed reflectivity and synthetic seismic trace of well 14-09 are shown in Figure 1. The amplitude spectrum of the calculated reflectivity is shown as figure 2. There is an obvious roll-off in the amplitude spectrum from 100 Hz to 0Hz, which indicates that the reflectivity is nonwhite. The high-frequency roll-off from 125 Hz to 250 Hz is due to an anti-alias filter used in the reflectivity calculation and is not an earth property. Figure 3 shows the Gabor spectrum of the nonwhite reflectivity, whose amplitude depends on both time and frequency. Here an initial time of 210 was employed to align well log data to the field data. This was estimated based on the depth data, velocity data and correlation between synthetic seismic trace and the field data. In general, the true reflectivity calculated from well 14-09 has obvious spectral and temporal color. As shown in Figure 4, the spectral color can be normalized with respect to time. The temporal color roughly tells how the magnitude of localized reflectivity changes with time, as illustrated by Figure 5.

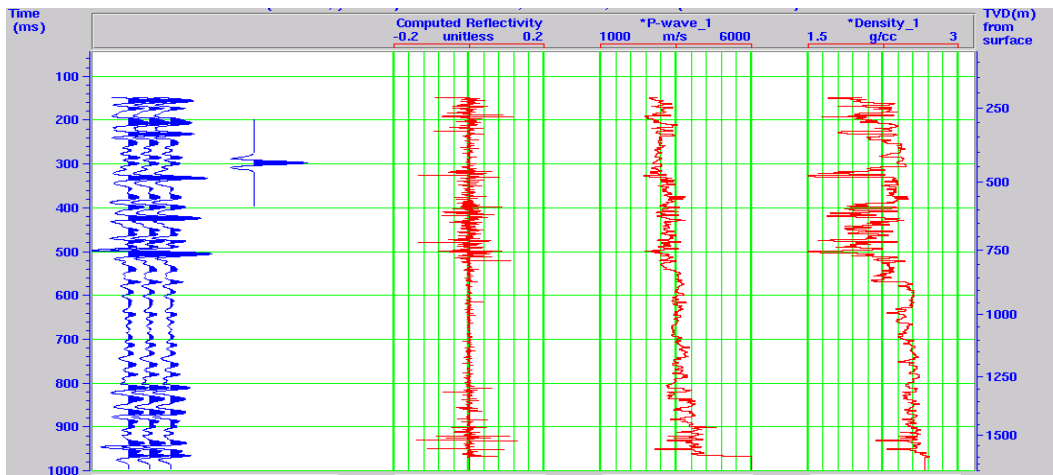


FIG. 1. well log 1409. From left to right: synthetic seismic trace, Ricker wavelet with a dominant frequency of 40Hz, computed reflectivity, P wave velocity and density.

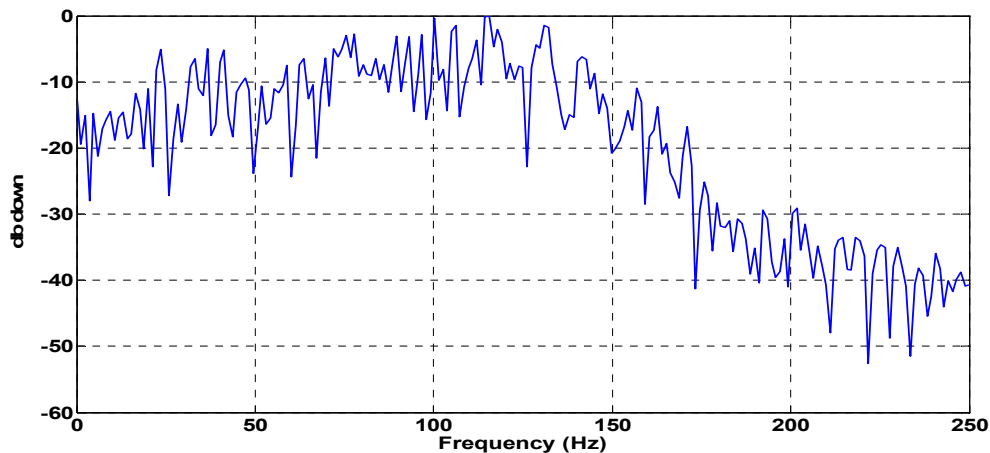


FIG. 2. The Fourier amplitude spectrum of the reflectivity shown in Figure 1.

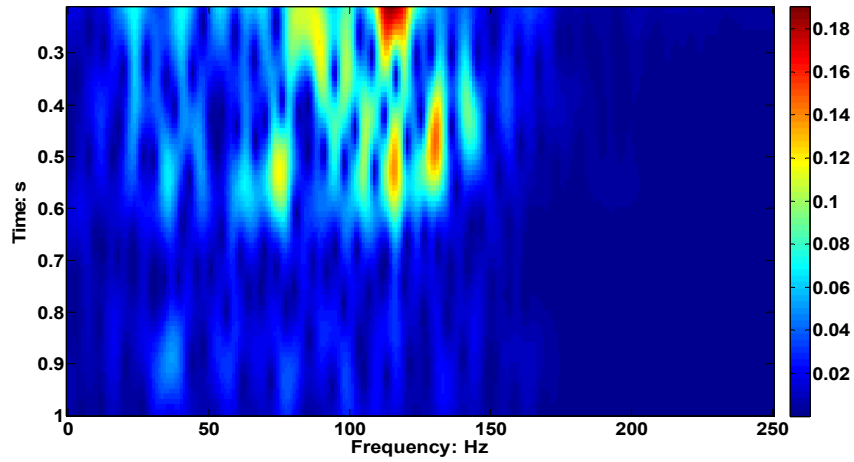


FIG. 3. Gabor amplitude spectrum of the nonwhite reflectivity shown in Figure 1.

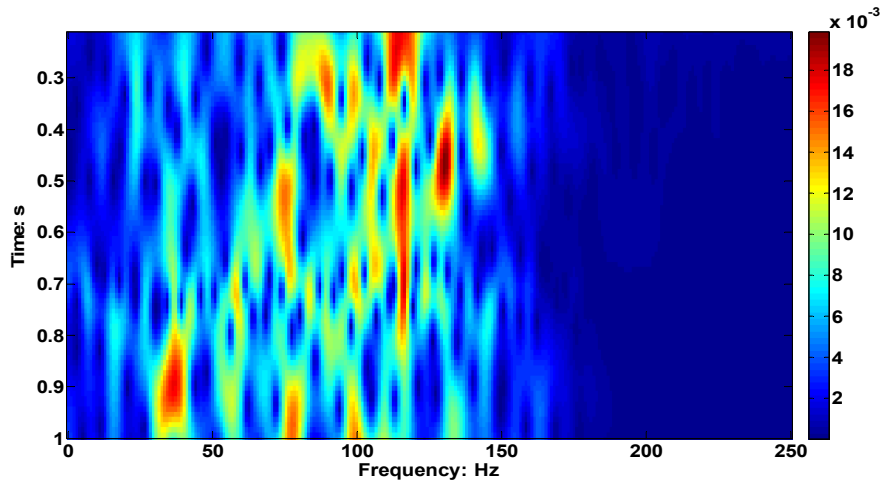


FIG. 4. Similar to Figure 3 except that each constant-time row of the Gabor amplitude spectrum has been independently normalized to remove the temporal variation. This emphasizes the spectral color of the nonwhite reflectivity shown in Figure 1.

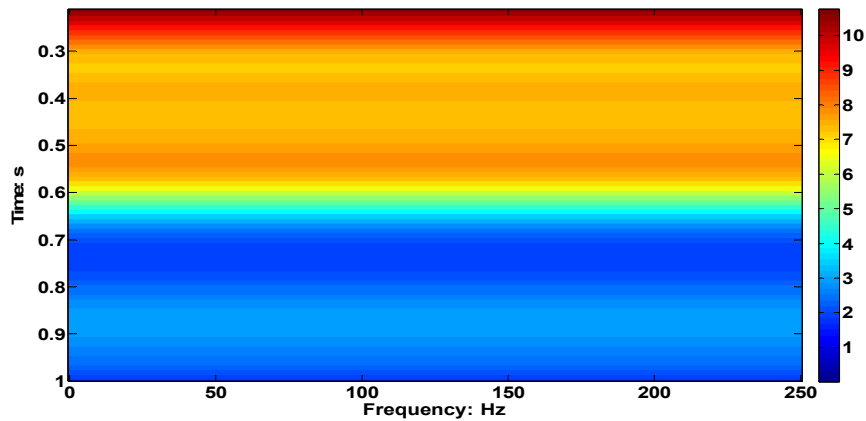


FIG. 5. The temporal variation of the Gabor spectrum shown in Figure 3. This emphasizes the temporal color of the nonwhite reflectivity shown in Figure 1.

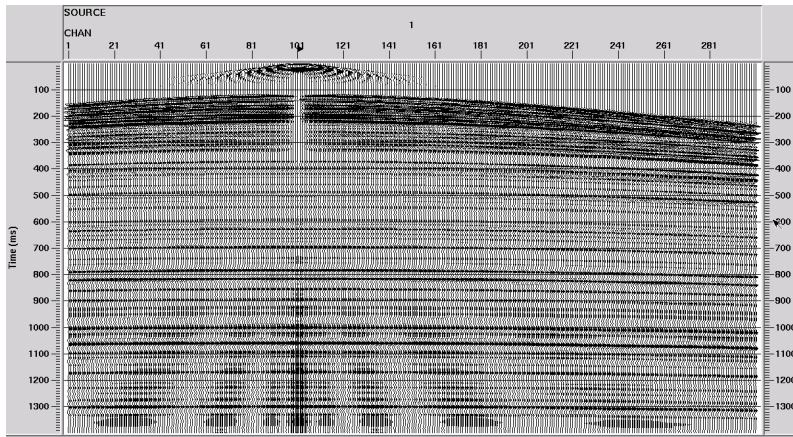


FIG. 6. Synthetic shot record created by Tiger software (AGC applied for display).

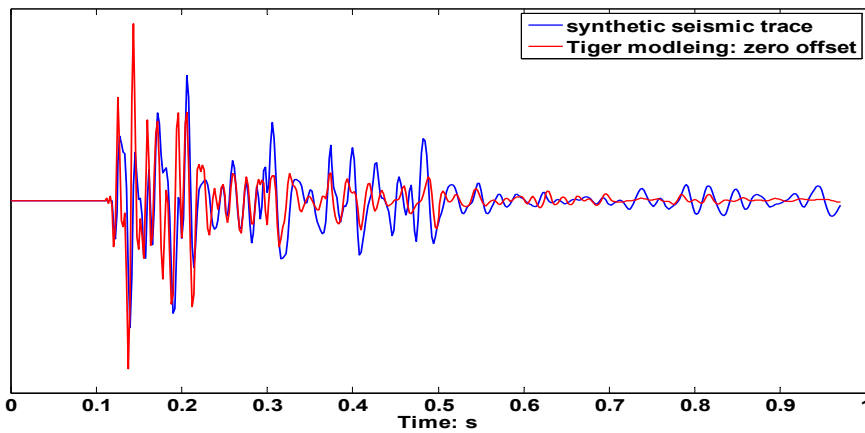


FIG. 7. Comparison of synthetic seismic traces. The blue curve is the synthetic 1D seismic trace; The red curve is the zero offset trace of Tiger modeling with first break removed and geometric spreading corrected.

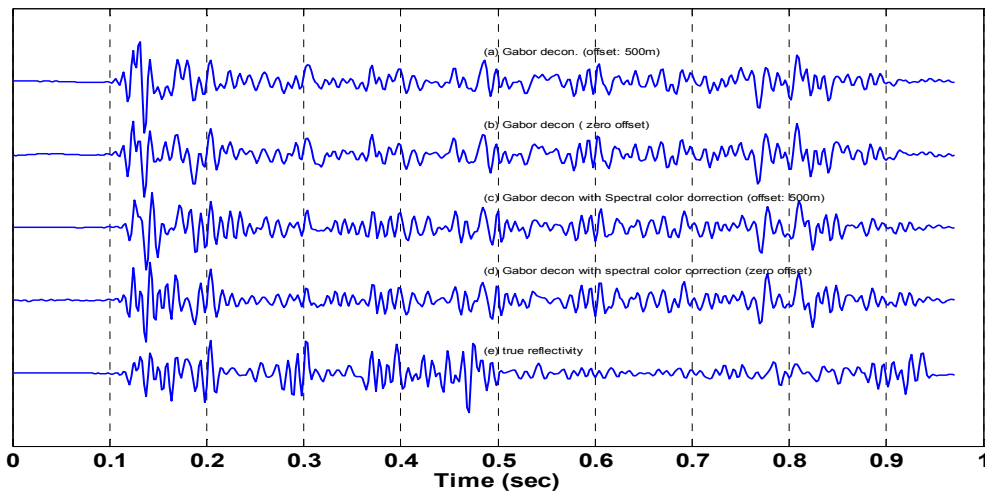


FIG. 8 Color correction. (a) Plain Gabor decon of the seismic trace with offset of 500m shown in Figure 6. (b) Plain Gabor decon of zero offset seismic trace shown in Figure 6. (c) Spectral color correction of the seismic trace with offset of 500m shown in Figure 6. (d) Spectral color correction of zero offset seismic trace shown in Figure 6. (e) True reflectivity.

Theoretically, color correction requires that the well log data and seismic trace should be aligned temporally. However, NMO stretch can be severe at far offsets and early times, which distorts the seismic wavelet and makes it not minimum phase. To address this problem, the Gabor deconvolution before NMO is applied with spectral color correction only. We use a synthetic shot record to test that spectral color correction is compatible with the alignment error of well log to seismic trace. A constant velocity of 5000m/s, constant Q of 50 and grid size of 5m x 5m were employed. The density model can be inverted from the well log reflectivity to make the earth model for seismic modeling consistent with our well log. Figure 6 show the synthetic shot record created by the Tiger finite-difference modeling software of SINTEF. For comparison a 1-D synthetic seismic trace was created in MATLAB using the well-log reflectivity, no multiples, and constant Q of 50 as well. A comparison of the 1D synthetic seismic trace and the zero offset seismic trace of Tiger modeling is shown as Figure 7. The reflection events match well from 0.1s to 0.4s, and there are obvious misfits from 0.42s to 0.55s. Gabor deconvolution with spectral color correction was applied to the zero offset trace and the trace with offsets of 500m respectively. Then, NMO is applied to the deconvolved trace with offset of 500m, and the final results and corresponding phase rotation are shown in Figure 8 and Figure 9 respectively. We can see that the deconvolution of zero offset and non-zero offset trace show similar results, except at early times, and the color correction gives better estimation with smaller phase rotation from 0.1s to 0.4s. Figure 7 and Figure 8 share similar misfit sections from 0.42s to 0.55s, which also manifest significant phase rotation. The reason for the misfit sections on deconvolved results and synthetic traces is not very clear, and may result from multiples included in Tiger modeling. Generally, Gabor deconvolution with color correction improves reflectivity estimation, and spectral color correction can accommodate the moveout of seismic traces adequately.

The Blackfoot seismic data were processed using ProMAX with a processing flow consisting of static correction, geometric spreading correction, prestack Gabor decon (with or without color correction), NMO, stacking, poststack Gabor decon (with or without color correction), and Kirchhoff time migration. To align the well log roughly with the field data, an initial time shift of 210ms, as mentioned previously, was applied to the well log data. For the plain Gabor deconvolution case, both prestack and poststack deconvolution were applied using conventional Gabor deconvolution. For the spectral color correction case, both prestack and poststack deconvolution were conducted using Gabor deconvolution with spectral color correction. For the full color correction case, Gabor deconvolution with spectral color correction and Gabor deconvolution with full color correction were used for prestack deconvolution and poststack deconvolution respectively. The migrated seismic data for these three cases are shown as Figure 10, Figure 11 and Figure 12. To compare the above results, some zoomed parts are shown from Figure 13 to Figure 15. From Figure 14, we can observe the separated events at 820 ms and 960ms, which are not clear in Figure 13. Compared with Figure 14, there is a lower amplitude zone around 700ms in Figure 15, which corresponds to the low amplitude zone around 0.7s in Figure 5.

To better understand color corrections in the frequency domain, a spectral analysis was conducted using the seismic data shown in Figure 10, Figure 11 and Figure 12. The average amplitude spectrum of the traces with CDP number from 50 to 250 and time

range from 500ms to 1500ms was calculated and compared with a synthetic trace computed from the well 14-09, as shown in Figure 16. The seismic data with color correction applied have higher amplitude for those frequency components over 30Hz. From the above comparison in time domain and frequency domain, we can see that spectral color correction strengthens the high frequency components of seismic data. Compared to spectral color correction, full color correction modifies the temporal amplitudes of the seismic trace according to well log information as well.

To track the variation of frequency band of seismic data during the data processing, using the spectral color correction case as an example, average amplitude spectra were calculated from seismic data after the application of prestack deconvolution, stacking, poststack deconvolution and migration. As shown in Figure 17, deconvolution whitens the seismic data to recover high frequency components, while stacking significantly de-whitens the spectrum of seismic data when it attenuates the noise. This is because deconvolution does not distinguish signal from noise and whitens the spectrum of signal plus noise. Since signal-to-noise ratios generally decrease with increasing frequency, stacking, which selectively attenuates noise, reduces the strength of high frequencies relative to low frequencies, thus de-whitening the spectrum. Kirchhoff Migration, which can be regarded as stacking along the diffraction curves, also de-whitens the seismic data; but the effect is less than stacking because noise is already reduced.

Color correction enriches the high frequency components of seismic data. To verify whether such an effect enhances the data or boosts the noise, it necessary to tie the migrated data to well log data. The target zone for the Blackfoot seismic data is around 1050ms, which corresponds to the end the well log. Considering the near surface part the seismic data is highly contaminated by noise, we use the lower part of the well log to tie the seismic data. The lower part of the well log is shown as figure 18. The synthetic seismic trace was created using a Ricker wavelet with a dominant frequency of 40Hz. In Figure 18, the last event of the synthetic seismic trace is generated by the single spike of the P wave velocity at the very end of well log, which is unrealistic because there are no later events. So, we use the events from 750ms to 950ms to correlate with the migrated data. According the X-Y coordinates of the well log location, the well log is mapped to the seismic trace of CDP 37 that has nearly the same X coordinate. The correlation of the synthetic trace to the migrated seismic data is shown as Figures 19, 20 and 21. We can see that the spectral color correction and full color correction have similar results. With color correction applied, the seismic data have higher frequency components for the events around 920ms and 950ms, all of which roughly match the synthetic seismic trace. For the correlation time range from 800ms to 1000ms, the phase rotation between the migrated seismic traces and synthetic seismic trace was measured and shown in Figure 22. The phase rotation for the spectral color correction case and full color correction case is similar and comparable to the conventional Gabor deconvolution case. So, with color correction applied, seismic data have more high frequency component and roughly tie better to the well log data. In other words, color correction can improve the resolution of our seismic data.

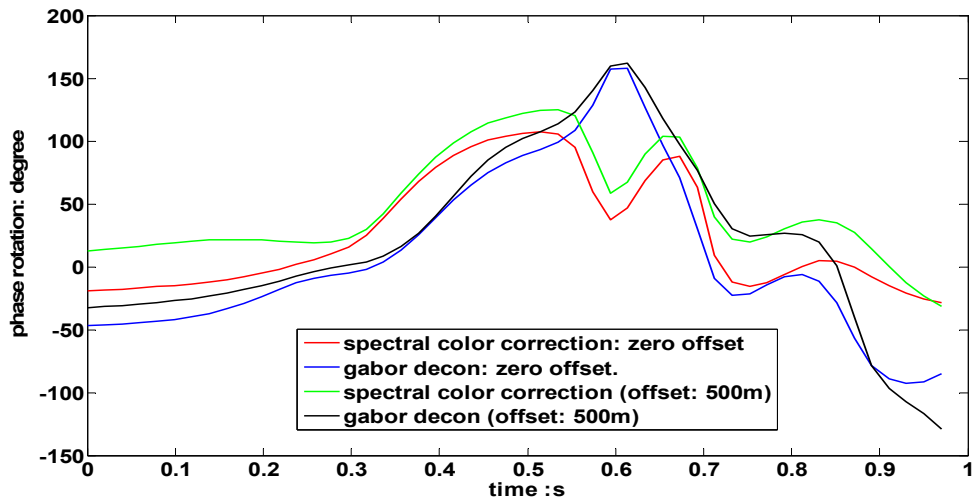


FIG. 9. Phase rotation measurement for the two reflectivity series shown in Figure 8.

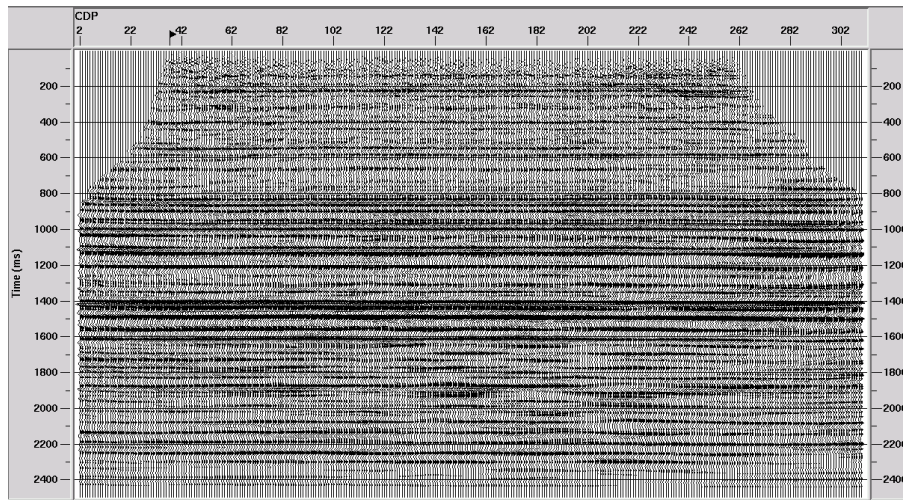


FIG. 10. Migrated seismic data with plain Gabor decon

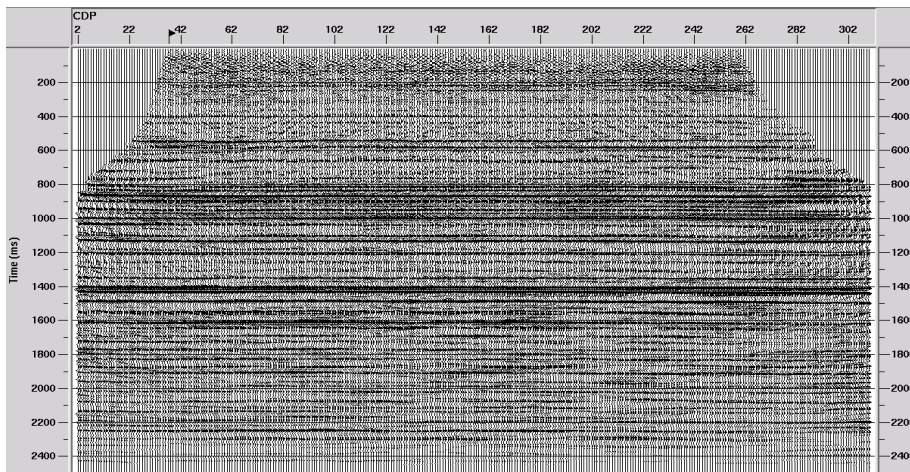


FIG. 11. Migrated seismic data with spectral color correction.

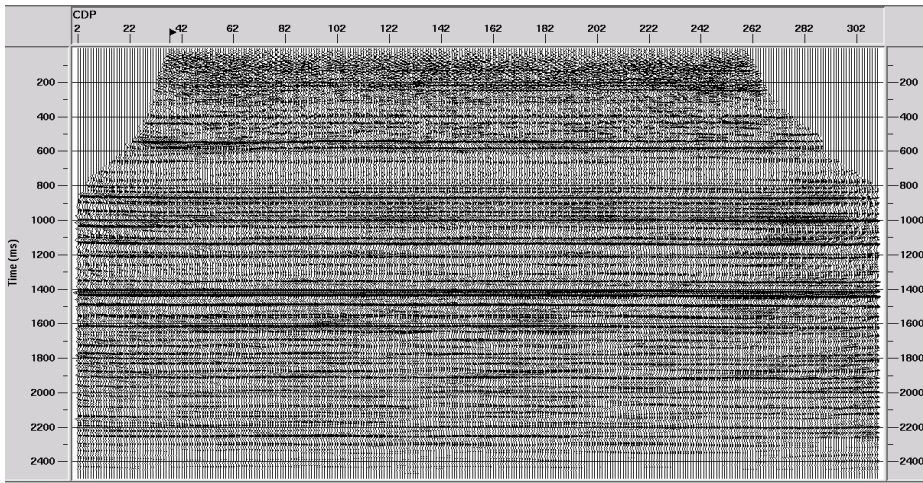


FIG. 12. Migrated seismic section with full color correction

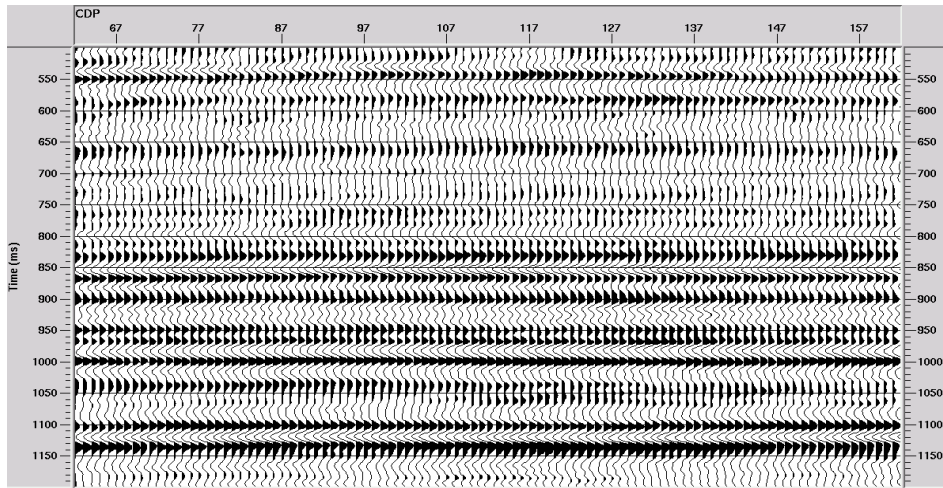


FIG. 13. A zoomed part of the seismic data shown in Figure 10.

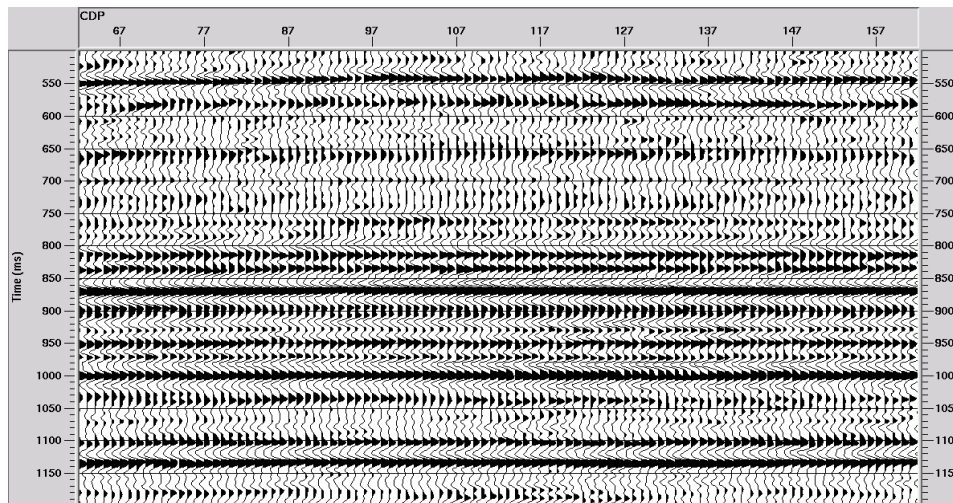


FIG. 14. A zoomed part of the seismic data shown in Figure 11.

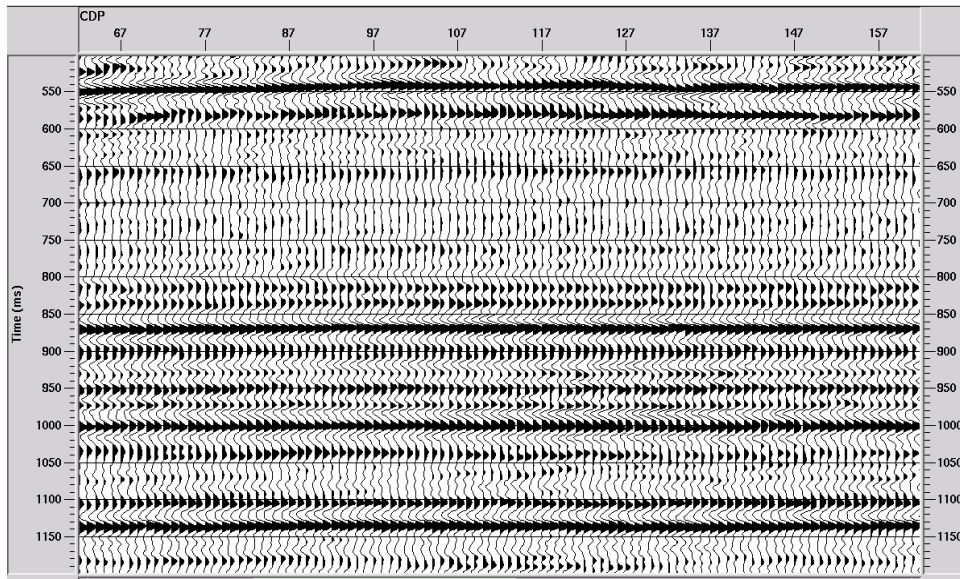


FIG. 15. A zoomed part of the seismic data shown in Figure 12.

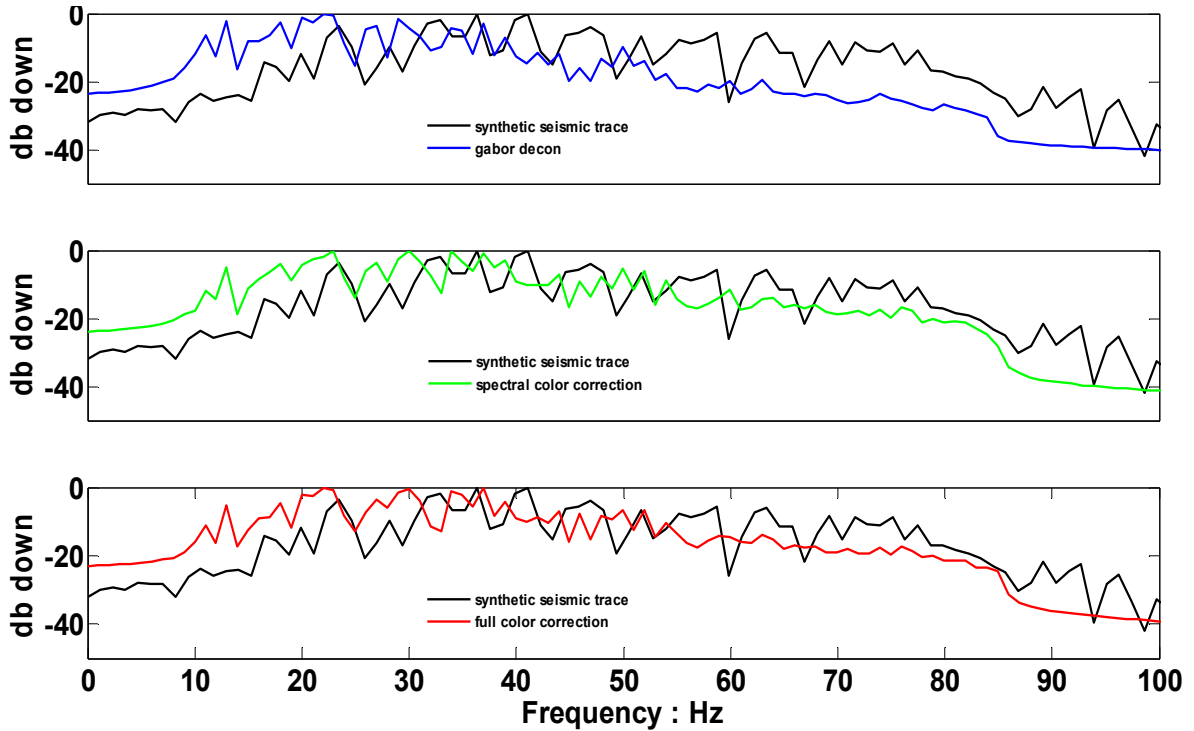


FIG. 16 The average amplitude spectra of the seismic data (CDP 50-250, time: 500ms-1500ms) shown in Figure 10 Figure 11 and Figure 12 and the amplitude spectrum of the synthetic seismic trace shown in Figure 1.

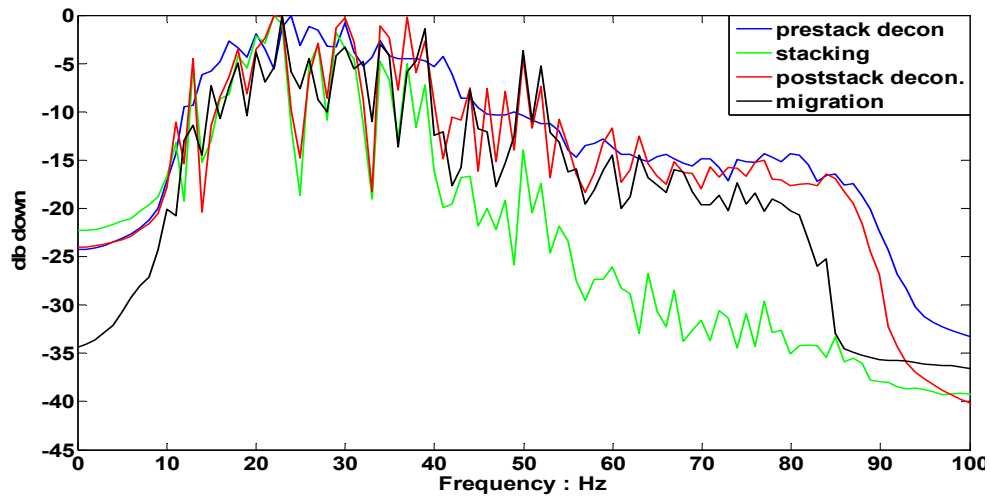


FIG. 17. The average amplitude spectra of seismic data at different stages of the data processing flow for the spectral color correction case. Blue: after prestack decon. (FFID: 7, CHAN 21-71, time: 800-1800ms); Green: after stacking (CDP 150-200, time: 500-1500ms); Red: after poststack decon. (CDP 150-200, time: 500-1500ms); Black: after Kirchhoff time migration (CDP 150-200, time: 500-1500ms).

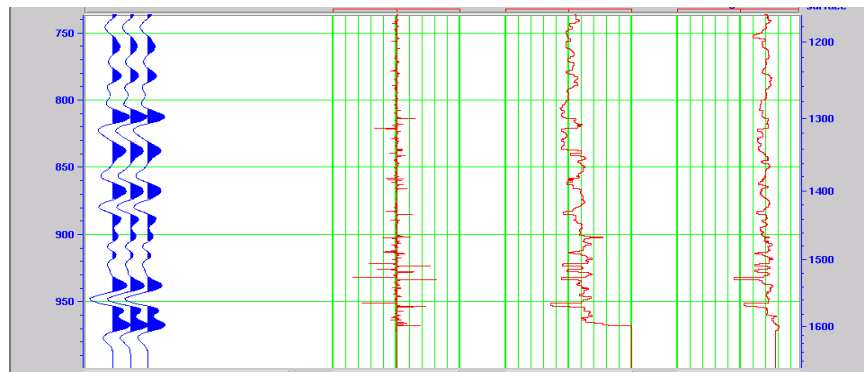


FIG. 18. Lower part the well 14-09. From left to right: synthetic seismic trace, computed reflectivity, P wave velocity and density.

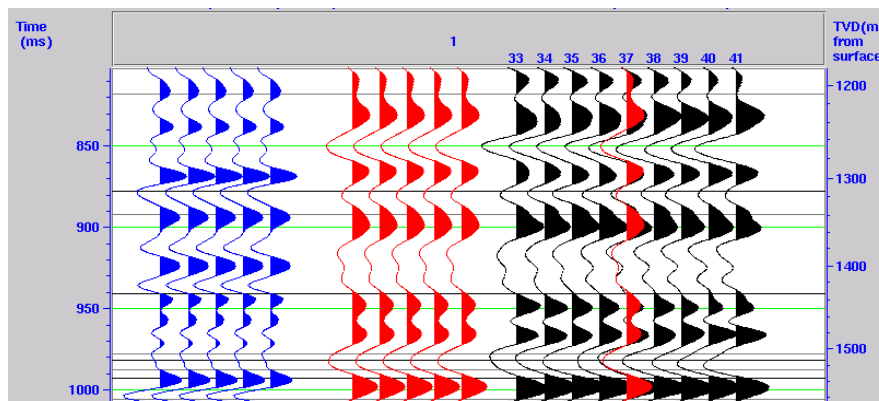


FIG. 19. Correlation of synthetic seismic trace and migrated seismic data with plain Gabor decon. Blue: synthetic seismic trace; Red: migrated seismic trace with CDP 37; Black: migrated seismic traces around CDP 37.

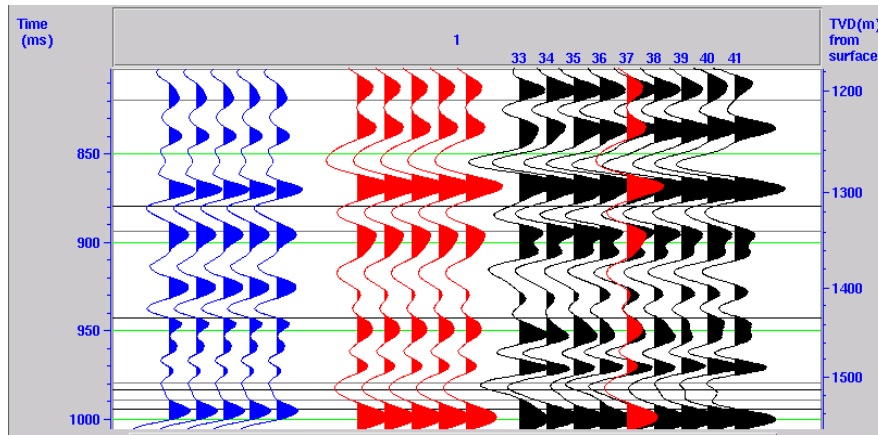


FIG. 20. Correlation of synthetic seismic trace and migrated seismic data with spectral color correction. Blue: synthetic seismic trace; Red: migrated seismic trace with CDP 37; Black: migrated seismic traces around CDP 37.

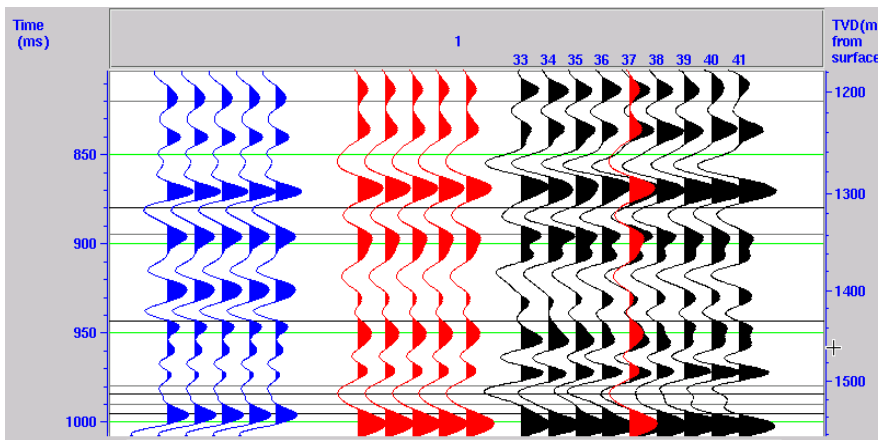


FIG. 21. Correlation of synthetic seismic trace and migrated seismic data with full color correction. Blue: synthetic seismic trace; Red: migrated seismic trace with CDP 37; Black: migrated seismic traces around CDP 37.

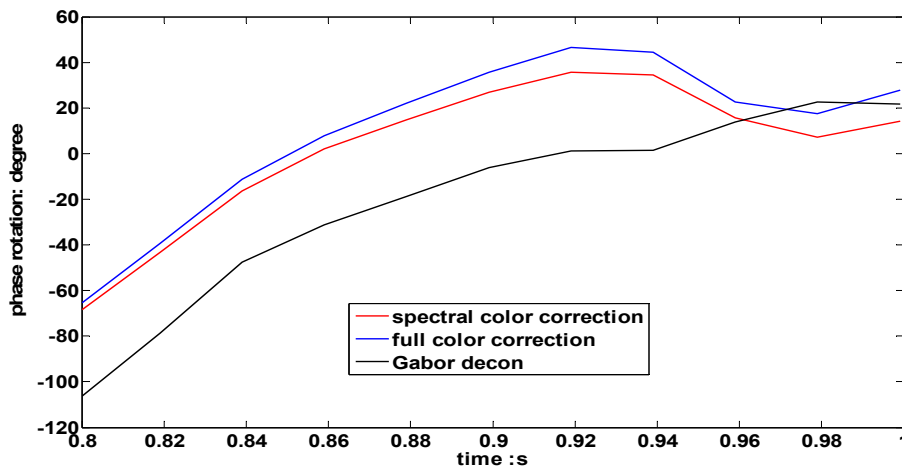


FIG. 22. Phase rotation between synthetic seismic trace and migrated seismic trace of CDP 37 from 0.8s to 1s.

CONCLUSION

In practice, the earth reflectivity function is usually nonwhite, and this color characteristic is time-variant, so seismic deconvolution needs to be corrected in a nonstationary way. If some reference well log information is available, color correction for Gabor deconvolution can be applied to shot records, which can improve reflectivity estimation. Deconvolution can whiten the spectrum of seismic data to recover high frequency components, while stacking and Kirchhoff time migration, at different levels, de-whiten the spectrum of seismic data. Testing on field data indicates that color correction can improve the resolution of seismic data, to some degree, and obtain a better tie to the well log data.

ACKNOWLEDGEMENTS

We thank Helen Isaac and Hanxing Lu for their help with Promax and Hampson Russell software, Faranak Mahmoudian for her help with Tiger modeling software, Kevin Hall and Rolf Maier for their IT support. In addition, the authors acknowledge the sponsors of CREWES project for their financial support.

REFERENCES

- Cheng, P. and Margrave, G.F., 2009, The influence of reflectivity color on Gabor deconvolution, CREWES 2009 research report, **21**.
- Cheng, P. and Margrave, G.F., 2008, Color correction for Gabor deconvolution, CREWES 2008 research report, **20**.
- Henley, D. C., Cheng, P. and Margrave, G. F., Earthtones: nonstationary color correction in ProMAX, CREWES 2010 research report, **22**.
- Margrave, G. F. and Lamoureux, M. P., 2002, Gabor deconvolution: CREWES Annual Research Report, 13.